

# MODULAR POWER COUPLERS FOR 217 MHZ SUPERCONDUCTING CH-CAVITIES

J. List<sup>1,2,4\*</sup>, K. Aulenbacher<sup>1,2,4</sup>, W. Barth<sup>1,2</sup>, M. Basten<sup>3</sup>, C. Burandt<sup>1,2</sup>, M. Busch<sup>3</sup>, F. Dziuba<sup>1,4</sup>, V. Gettmann<sup>1,2</sup>, M. Heilmann<sup>2</sup>, T. Kürzeder<sup>1,2</sup>, S. Lauber<sup>1,2,4</sup>, M. Miski-Oglu<sup>1,2</sup>, H. Podlech<sup>3</sup>, A. Schnase<sup>2</sup>, M. Schwarz<sup>3</sup>, S. Yaramyshev<sup>2</sup>

<sup>1</sup>HIM, Helmholtz Institute Mainz, 55099 Mainz, Germany

<sup>2</sup>GSI Helmholtzzentrum, 64291 Darmstadt, Germany

<sup>3</sup>IAP, Goethe-University Frankfurt, 60438 Frankfurt am Main, Germany

<sup>4</sup>IKP, Johannes Gutenberg-University Mainz, 55128 Mainz, Germany

## Abstract

The HELmholtz LInear ACcelerator (HELIAC) is being developed by a collaboration of HIM, GSI and the IAP. It is a superconducting (sc), continuous wave (cw) heavy ion linac that comprises novel Crossbar H-mode (CH) cavities. In April 2017 and November/December 2018 the first sc CH-cavity of the linac was tested with beam. The first operations of the cavity showed, that the prototype of the rf power coupler needs to be further improved. A new version of the coupler is being designed at the HIM. The development will mainly be focused on the reduction of heat input into the cryostat caused by the coupler. Also the coupler will have a modular design. This improves the accessibility and maintenance of the coupler. Various cryogenic- and rf tests are foreseen to provide a reliable, fail-safe coupler for the HELIAC. For an enhanced coupler test stand a movable reflector has been designed and built. With its movable semi-reflective element, it allows to operate the test stand in a resonance mode. In addition, the movable reflector can vary the coupling factor. This contribution discusses the recent coupler R&D for the HELIAC.

## INTRODUCTION

The UNiversal Linear ACcelerator (UNILAC) at the GSI will be upgraded and used as an injector for the Facility for Antiproton and Ion Research (FAIR) [1,2]. After the upgrade the UNILAC will no longer be suitable for the Super Heavy Element (SHE)-research program [3] and other UNILAC-users as the material research at GSI.

For this purpose the sc cw HELIAC is being built at GSI, to accelerate heavy ions up to 7.3 MeV/u [4,5]. It comprises Crossbar-H-mode (CH) RF cavities, originally developed at IAP [6]. The first cavity of the HELIAC (CH0) was successfully tested with beam in summer 2017 [7,8] and late 2018 [9,10] within the Demonstrator project. This is the first sc CH-cavity worldwide tested and operated with heavy ion beam. In the next stage an advanced cryo module comprising three CH-cavities [11], a rebuncher [12,13] and two solenoids will be set up for further testing. This module serves as a first of series for three additional similar modules

(Fig. 1) to complete the entire HELIAC [14]. The heavy ion beam is provided by the GSI - High Charge State injector /HochLadungsInjektor (HLI).

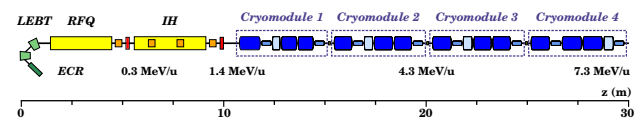


Figure 1: Recent design of the cw-LINAC at GSI made with four standard cryomodules.

## POWER COUPLERS

In previous tests with the CH0 a capacitive power coupler, described in [15,16], was used for the HELIAC. A high static heat load of the coupler to the cryostat has been observed, as well as a major heat dissipation at the windows [17]. Due to thermic stress one of the two ceramic coupler windows was leaking.

This prompted the decision to revise the design of the coupler.

The design criteria for the revised coupler design are:

- High reliability, especially of the windows
- Easy to clean, easy to maintain
- 5 kW maximal forward power
- Low static and dynamic heatload
- Low reflection at 216.816 MHz

The coupler design is based on a  $3\frac{1}{8}$  inch rigid coaxial line and transmits to the diameter of the cavity's coupler port of 14 mm. Two RF windows are situated in the line.

The coupler will have a modular design, as shown in Fig. 2. This has the advantage, that any part of the coupler can be replaced easily and inexpensively in case of failure, as the remaining part of the coupler stays untouched. This is particularly true for the windows, which are the most delicate part of the coupler. Also the assembly can be cleaned very comfortably in the cleanroom of the HIM [18]. Each window is integrated in a double-sided CF 100-flange (see Fig. 3).

\* j.list@gsi.de



Figure 2: New modular design of the power coupler with two window-flanges.

The technological difficult connection of the ceramic to the steel of the outer conductor is realized by an u-shaped spring.

The window houses a jack for a standard  $3\frac{1}{8}$  inch connector (the connector is depicted in silver in Fig. 3) for an attachment of the inner conductor. Mounted onto the cold window is a cooling pipe that will be connected to the helium shield of the cryostat, acting as a thermic intercept. Two prototypes of these flanges are in production right now, built by Friatec [19].

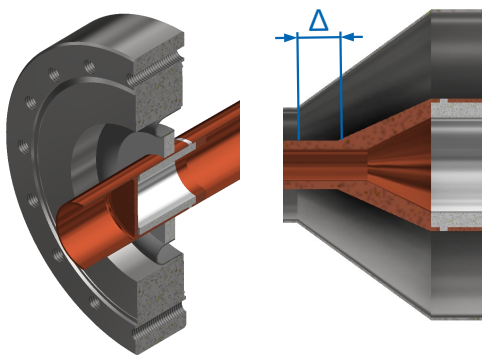


Figure 3: Window-Flange with ceramic window, u-shaped spring and connection jack with inner conductor mounted to one side (left side); conical adjustment of diameter transition from  $3\frac{1}{8}$ '' to 14 mm rigid line (right side).

The diameter transition is realized by a conical adjustment. A conical diameter transition causes a parasitic capacity. This is canceled out by an additional inductivity, that is induced by a shift  $\Delta$  between the diameter transition of the inner and outer conductor (see Fig. 3).

A bellow with a stroke of 20 mm is foreseen to absorb thermic stress and vary the coupling factor  $\beta$  in a wide range. The latter is important for the commissioning process of the HELIAC, so the stroke will possibly be changed in the future.

To cope with the static heat input, the wall thickness of the conductors will be decreased to the technical possible



Figure 4: Ceramic-metal connection used for the HELIAC-coupler by the GSI-workshop (left) and by Friatec (right).

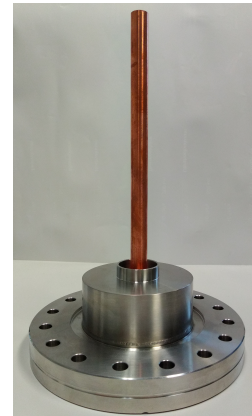


Figure 5: Cold part of the former coupler design recently built in the GSI workshop.

minimum. The inner conductor of the previous coupler design is made of copper. It is foreseen to change the material to steel with a copper coating for lower heat transfer and good RF properties. The heat dissipation of the former coupler, described in [17], was most likely caused by the TiN-coating of the windows. The future coupler window will not be TiN coated, which could be added later, if necessary.

Meanwhile the GSI technological laboratory is working on an alternative solution (Fig. 4) for the ceramic-metal-connection of the windows. In a first step the cold part of the former coupler design [15] was recently rebuilt by the GSI workshop (Fig. 5). In a test it was cooled down to 4 K, without evincing leakage. Furthermore, it will undergo an RF test. If this is a success, an alternative window flange will be developed, that matches the RF reflection-coefficient of the window-flange above. So both flanges could be interchanged equally.

## COUPLER RF DESIGN

One of the most important points of the RF design is the optimization of the window-distance. For certain distances the reflection is minimal. In addition, the conical diameter adjustment of the coupler needs to be optimized. These two design-parameters are interconnected and must be adjusted iteratively. The dimensions of couplers have been evaluated with CST Microwave Studio Suite [20] and cross checked with a S-matrix calculation, using Wolfram Mathematica [21].

Content from this work may be used under the terms of the CC BY 3.0 licence (© 2019). Any distribution of this work must maintain attribution to the author(s), title of the work, publisher, and DOI.

### RF Design with CST Microwave Studio Suite

The design-goal of the simulation was a minimal  $S_{11}$ -Parameter at the HELIAC's resonance frequency of 216.816 MHz. For this, the window distance and the dimensions of the conical adjustment were varied.

In Fig. 6  $S_{11}$  and  $S_{21}$  of the coupler after optimization are depicted. At the resonance frequency  $S_{11}$  becomes approximately  $-70$  dB.

Inside a range of  $\pm 45$  MHz the reflection does not exceed  $-20$  dB.

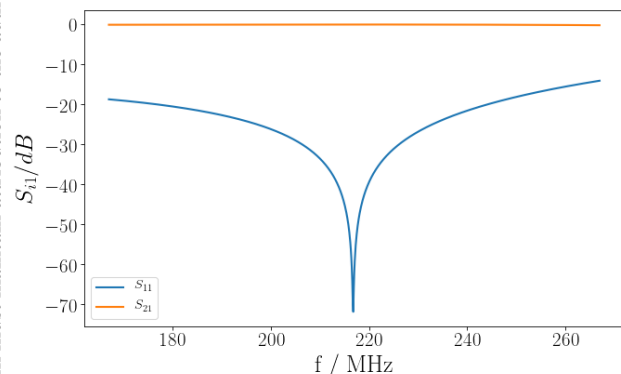


Figure 6: S-Parameters of the coupler after optimization.

### RF studies with S-Matrices

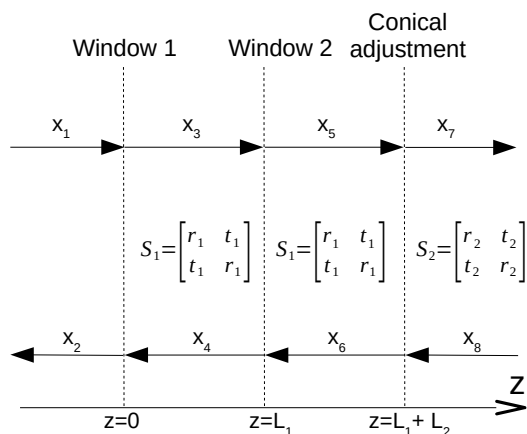


Figure 7: Diagram of the power coupler with two RF windows and a conical diameter adjustment represented by an S-matrix calculation. An S-matrix with a reflection and a transmission coefficient is assigned to both windows ( $S_1$ ,  $r_1$ ,  $t_1$ ) and the diameter adjustment ( $S_2$ ,  $r_2$ ,  $t_2$ ). The windows are positioned in a distance  $z = 0$  and  $z = L_1$ , the diameter transition at the position  $z = L_1 + L_2$ .

The coupler has been also studied with an S-matrix calculation using Mathematica. Since the examined part of the coupler is a coaxial waveguide with a TEM-mode, the

problem can be regarded as 1-dimensional. In this approach the windows as well as the conical adjustment are treated as a semi-permeable mirror with a reflection-coefficient  $r$  on an axis  $z$ . With this an S-matrix can be assigned to each element. Thus they follow the S-matrix formalism of a two-port network:

$$\vec{b} = S\vec{a} \quad (1)$$

with the incoming waves described by the vector  $\vec{a}$  and the originating waves by the vector  $\vec{b}$ . The coupler is represented as a system of three linked matrix-equations as in Eq. 1 with the waves  $x_{1-8}$  (Fig. 7). Using the characteristics of the S-matrix and the connecting conditions, these matrices can be written as:

$$S = \begin{pmatrix} -r(f) e^{i\phi_r} & i \sqrt{1-r(f)^2} e^{i\phi_r} \\ i \sqrt{1-r(f)^2} e^{i\phi_r} & -r(f) e^{i\phi_r} \end{pmatrix} \quad (2)$$

with the frequency-dependent reflection-coefficient  $r(f)$  and the phase at the reflecting element:

$$\phi_r = -\arctan\left(\frac{\sqrt{1-r(f)^2}}{r(f)}\right). \quad (3)$$

The reflection-coefficient-curve  $r(f)$  of the windows and the conical adjustment is imported from a CST Microwave Studio simulation.

The system of equations was solved with Wolfram Mathematica. With this the resulting reflection coefficient  $\widehat{S}_{11}$  of the whole coupler at the input-port could be evaluated.

In Fig. 8  $|\widehat{S}_{11}|^2$  is compared with the results from the CST-Microwave Studio simulation. The blue line shows the curve evaluated by CST, the orange line the curve evaluated by Mathematica. The curves match properly in the region of interest (0–500 MHz).

Figure 8 shows that these S-matrix models can provide a quick, relatively accurate result, in contrast to time consuming but more precise CST simulations. Hence they are suitable for a first estimation.

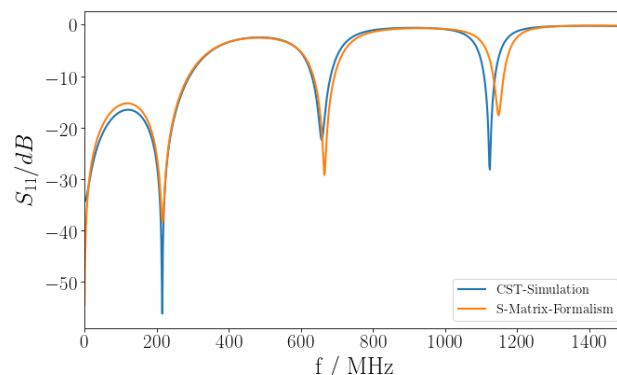


Figure 8: Comparison of the  $|\widehat{S}_{11}|^2$ -curve evaluated by CST and Mathematica.

## Distance of Windows to Cavity

In order to prevent additional dielectrical losses at the coupler windows, high electrical fields at their position have to be avoided.

The electrical field depends strongly on external coupling and beam loading of the cavity. The most efficient case, in terms of rf power usage, would be a pure traveling wave. While this is in principle the case for a matched load, the HELIAC cavities will be overcoupled, keeping the power necessary to compensate microphonic detuning as low as possible [22]. This causes a standing wave in the coupler.

Until a cw injector is realized, the HELIAC uses the HLI as injector, operated with a max. duty factor of 25 %. Since all the HELIAC cavities are operated in cw mode, it is reasonable to optimise the coupler for a given  $\beta$  but no beam load (The beam is turned off 75 % of the time).

For a first estimation of the distance between the windows and the cavity, a model using S-matrices similar to the previous chapter is set up. The coupler is represented as before. The S-parameters of a cavity can be expressed by [23]:

$$S_{ii} = 1 + i \frac{\Gamma_i}{f - f_0 - i \frac{\Gamma}{2}} \quad (4)$$

$$S_{ij} = i \frac{\sqrt{\Gamma_i \Gamma_j}}{f - f_0 - i \frac{\Gamma}{2}}, \quad (5)$$

where  $\Gamma = \Gamma_1 + \Gamma_2 + \Gamma_\Omega + \Gamma_{beam}$  is the resonance width of the loaded system,  $\Gamma_1$  of the input coupler,  $\Gamma_2$  of the output coupler,  $\Gamma_\Omega$  of the losses in the cavity and  $\Gamma_{beam}$  of the beam.  $f_0$  is the resonance frequency of the cavity.

The cavity is now placed in a distance  $L_c$  from the coupler window. An interactive plot (Fig. 9) was created in Mathematica. The plot shows the electrical field inside the coupler in space and time. The input field has the amplitude of 1. By changing the distance  $L_c$ , the coupling factor  $\beta$  or the beam current the electrical field is then updated interactively. With this, a first estimation of the cavity-window-distance can be determined. Of course this must be verified and studied in greater detail in a CST Microwave Studio simulation. Studies are currently ongoing.

## SUMMARY

An advanced coupler design for the HELIAC has been presented. The coupler consists of several modules. Thus, the cleaning process and maintenance is eased. An RF window-flange has been designed, a double-sided CF100-flange containing a ceramic window. Two prototypes are built right now by Friatec. The GSI workshop is working on an alternative in house design to provide for proper ceramic-metal-connection. Recently, a part of the former coupler design was rebuilt. In future, it is foreseen to build an own version of the window-flange in parallel. Both flanges will be designed in a way that they are interchangeable.

RF simulations have been conducted to optimize the window distance and the dimensions of the diameter translation. Mathematical models were constructed, using the S-matrix

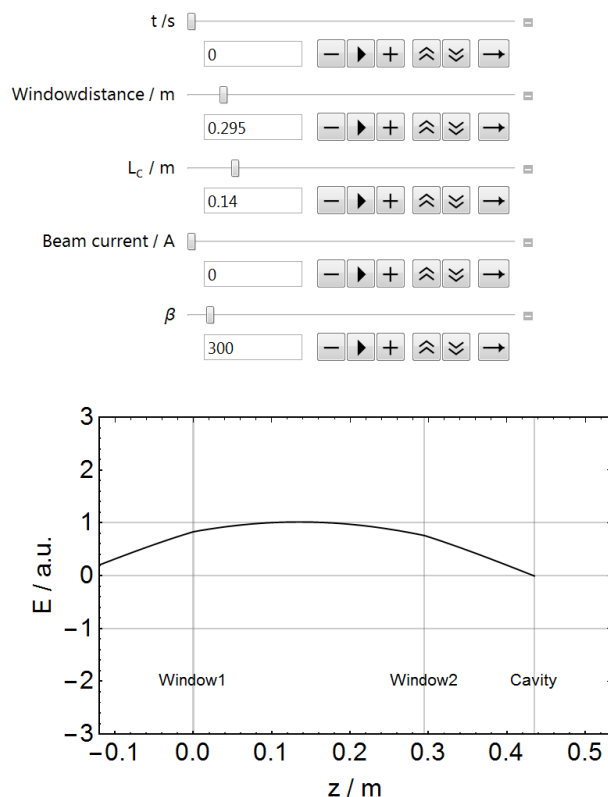


Figure 9: Screenshot of the interactive plot depicting the electrical field in the coupler, when attached to cavity. The distance of the window to the cavity  $L_c$ , the beam current and the coupling factor  $\beta$  can be varied. The plot automatically updates the field distribution in the coupler.

formalism. With this, the coupler was modelled analytically and an  $S_{11}$ -curve was evaluated and compared with the results of the CST Microwave Studio Suite. Both curves are in good agreement. Also, a first estimation of the distance of the coupler-windows to the cavity could be evaluated by such a model. This has to be confirmed and inspected closer with a CST simulation.

## OUTLOOK

It is intended to finish a first prototype of the coupler by the end of this year. The window-flanges will undergo a liquid helium leak test. After this, an RF power-test of the whole coupler will be conducted.

The design of a movable reflector (MR), already successfully used at Fermilab [24], was adapted to the HELIAC's frequency of 217 MHz and constructed at the GSI workshop. As proposed in [24], the MR can be used in a coupler test stand to create a resonance condition. With this, the maximal electrical fields can be increased. Furthermore, studies on the interaction of cavity and the movable reflector are ongoing on at the moment.

## ACKNOWLEDGEMENTS

The coupler R& D is strongly supported by the GSI technology laboratory and the GSI workshop. The cryogenic tests of the in house coupler part was planned and heavily supported by P. Kowina and T. Reichert of the GSI Ring Instruments department.

## REFERENCES

- [1] W. Barth *et al.*, "Upgrade program of the high current heavy ion UNILAC as an injector for FAIR", *Nucl. Instr. Meth. Phys. Res. Sect. A*, vol. 577, no. 1-2, pp. 211–214, Jul. 2007, doi:10.1016/j.nima.2007.02.054.
- [2] W. Barth *et al.*, "High brilliance uranium beams for the GSI FAIR", *Phys. Rev. ST Accel. Beams*, vol. 20, p. 050101, May 2017 DOI:10.1103/PhysRevAccelBeams.20.050101.
- [3] J. Khuyagbaatar *et al.*, " $^{48}\text{Ca} + ^{249}\text{Bk}$  Fusion reaction leading to element  $Z=117$ : long-lived  $\alpha$ -decaying  $^{270}\text{Db}$  and Discovery of  $^{266}\text{Lr}$ ", *Phys. Rev. Lett.*, vol. 112, no. 17, p. 172501, May 2014.
- [4] M. Schwarz *et al.*, "Beam dynamics simulations for the new superconducting CW heavy ion LINAC at GSI", *J. Phys. Conf. Ser.*, vol. 1067, p. 052 006, 2018. doi: 10.1088/1742-6596/1067/5/052006.
- [5] S. Yaramyshev *et al.*, "Advanced approach for beam matching along the multi-cavity SC CW linac at GSI", *J. Phys. Conf. Ser.*, vol 1067, 052005, 2018 DOI:10.1088/1742-6596/1067/5/052005.
- [6] H. Podlech *et al.*, "Superconducting CH structure", *Phys. Rev. ST Accel. Beams*, vol. 10, p. 080101, 2007, doi: 10.1103/PhysRevSTAB.10.080101.
- [7] W. Barth *et al.*, "First heavy ion beam tests with a superconducting multigap CH cavity", *Phys. Rev. Accel. Beams*, vol. 21, p. 020 102, 2 2018. doi: 10.1103/PhysRevAccelBeams.21.020102.
- [8] W. Barth *et al.*, "Superconducting CH-Cavity heavy ion beam testing at GSI", *J. Phys. Conf. Ser.*, vol. 1067, p. 052 007, 2018. doi: 10.1088/1742-6596/1067/5/052007.
- [9] M. Miski-Oglu *et al.*, "Beam Commissioning of the Demonstrator Setup for the Superconducting Continuous Wave HIM/GSI-Linac", presented at the IPAC'19, Melbourne, Australia, May 2019, paper MOZZPLM1, this conference.
- [10] F. D. Dziuba *et al.*, "Further RF Measurements on the Superconducting 217 MHz CH Demonstrator Cavity for a CW Linac at GSI", presented at the IPAC'19, Melbourne, Australia, May 2019, paper WEPRB014, this conference.
- [11] M. Basten *et al.*, "Cryogenic Tests of the Superconducting =0.069 CH-cavities for the HELIAC-project", in *Proc. LINAC'18*, Beijing, China, Sep. 2018, pp. 855–858. doi: 10.18429/JACoW-LINAC2018-THP0072
- [12] M. Gusarova *et al.*, "Design of the two-gap superconducting re-buncher", *J. Phys. Conf. Ser.*, vol. 1067, p. 082005, Oct. 2018 DOI:10.1088/1742-6596/1067/8/082005.
- [13] K. Taletskiy *et al.*, "Comparative study of low beta multi-gap superconducting bunchers", *J. Phys. Conf. Ser.*, vol. 1067, p. 082006, Oct. 2018 DOI:10.1088/1742-6596/1067/8/082005.
- [14] T. Conrad *et al.*, "Cavity Designs for the CH3 to CH11 of the Superconducting Heavy Ion Accelerator HELIAC", presented at the SRF'19, Dresden, Germany, Jun.-Jul. 2019, paper TUP005.
- [15] R. Blank, "Entwicklung eines 217 MHz Hochleistungskopplers für das cw-LINAC-Demonstrator Projekt", *Master's thesis*, Goethe-University Frankfurt 2015.
- [16] M. Heilmann *et al.*, "High Power RF Coupler for the CW-Linac Demonstrator at GSI", in *Proc. IPAC'17*, Copenhagen, Denmark, May 2017, pp. 990–992. doi : 10.18429/JACoW-IPAC2017-MOPVA054
- [17] J. List *et al.*, "High Power Coupler R&D for Superconducting CH-cavities", in *Proc. LINAC'18*, Beijing, China, Sep. 2018, pp. 920–923. doi:10.18429/JACoW-LINAC2018-THP0107
- [18] T. Kuerzeder *et al.*, "Commissioning of a Cleanroom for SRF Activities at the Helmholtz Institute Mainz", presented at the SRF'19, Dresden, Germany, Jun.-Jul. 2019, paper THP101.
- [19] FRIATEC GmbH (June. 17, 2019), [www.friatec.de](http://www.friatec.de)
- [20] CST-Computer Simulation Technology AG. (June. 17, 2019), <https://www.cst.com/products/cstmws>
- [21] Wolfram Research, Inc., Mathematica, Version 12.0, (June. 17, 2019) , <http://www.wolfram.com/mathematica/>
- [22] C. Burandt *et al.*, "Considerations for Efficient RF Operation for the Advanced cw-Linac Demonstrator at GSI", presented at the SRF'19, Dresden, Germany, Jun.-Jul. 2019, paper MOP081.
- [23] H. Alt *et al.*, "Gaussian orthogonal ensemble statistics in a microwave stadium billiard with chaotic dynamics: Porter-Thomas distribution and algebraic decay of time correlations", *Phys. Rev. Lett.*, vol. 74, pp. 62–65, 1995.
- [24] S. Kazakov, B. M. Hanna, and O. V. Pronitchev, "Testing of 325 MHz Couplers at Test Stand in Resonance Mode", in *Proc. SRF'15*, Whistler, Canada, Sep. 2015, paper THPB098, pp. 1376–1378.